NUMERICAL SCHEMES FOR PARAMETRIZATIONS

A.C.M. Beljaars
European Centre for Medium Range Weather Forecasts
Reading, UK

1. INTRODUCTION

Sub-grid processes play an important role in numerical weather prediction models and climate models. Development of parametrizations has been a major research activity for many years and has resulted in considerable reduction of systematic model errors and improved forecast skill in the medium range. Direct output from the parametrized sub-grid processes such as surface fluxes, precipitation, cloudiness and 2 m temperature has become an important forecast product in the short range and will become an essential ingredient of the data assimilation cycle.

However, the development of numerical schemes to solve the parametrized part of the equations has received relatively little attention. The main reason is that the parametrizations are often thought to be too inaccurate to justify sophisticated and generally more expensive numerical methods. So the accuracy of the method is generally not considered and the conservative property and stability of the scheme remain the dominant concerns. Inaccuracies of the numerical scheme (e.g. truncation errors in time and space) are often concealed by problems in the parametrization. With the numerical solver as part of the parametrization it can happen that improved resolution or a more accurate scheme leads to lower quality of the forecast. In principle it is better to isolate the parametrization problem from the numerical technique, but we will see that this is not always possible.

In section 2 of this paper we will give an overview of the numerical techniques that are used for the parametrized parts of the equations in the ECMWF model and describe the general philosophy behind it. The methods are generally different for different processes. Recent developments in the numerical treatment of the vertical diffusion will be discussed in section 3.

It illustrates some of the problems that arise from process splitting, which is relevant to all the physical processes. In section 4, we will discuss the diffusion of moisture and heat in the soil. This is an example of a scheme where the accuracy of the numerical method is rather poor, but where numerical errors are probably still smaller than the parametrization errors.

2. OVERVIEW OF THE NUMERICAL METHODS USED FOR THE PARAMETRIZED PARTS OF THE EQUATIONS IN THE ECMWF MODEL

The time integration scheme used for the different parametrized sub-grid processes is based on the following simple ideas:

- The scheme has to be compatible with the time integration of the adiabatic part of the model. The ECMWF model uses leapfrog time integration combined with time filtering. The latter is necessary to avoid decoupling between the even and uneven time steps.
- The tendencies due to different processes are computed separately enabling a modular software design and the possibility of different methods for different processes. We will call this procedure "process splitting", when the increments due to different processes are completely independent. When function values are incremented with one process and the next process starts from these intermediate values, we call it the "method of fractional steps". Both principles are used.
- Explicit schemes are used if possible. In case of stability problems, the scheme is made as implicit as necessary to guarantee stability.

We explain the procedure with the equation for variable Ψ, which can be one of the horizontal wind components U, V, temperature T or specific humidity Q:

$$\frac{\partial \Psi}{\partial t} = D_\Psi + P_\Psi \,, \qquad (1)$$

where D_Ψ symbolizes the dynamic tendency (including advection) and P_Ψ the tendency due to parametrized processes. The latter can be divided into radiation R, vertical diffusion VD, gravity wave drag GWD, convection (shallow and penetrative) C, and large scale precipitation LSP:

$$P_\Psi = R_\Psi + VD_\Psi + GWD_\Psi + C_\Psi + LSP_\Psi \ . \qquad (2)$$

The time integration can be in spectral or grid point space. In the ECMWF model some terms of the dynamics are computed in the spectral domain, others are evaluated in grid space. In this section we will limit computations to grid space.

With time discretized as $t = n\Delta t$, each step of the leapfrog scheme involves a time integration from n-1 to n+1 where the right hand side of the equation is evaluated at time level n (the semi-implicit treatment of the gravity wave part and advection of vorticity and moisture has been neglected here). For the adiabatic part only, the integration from $(n-1)\Delta t$ to $(n+1)\Delta t$ gives an increment of

$$\Delta\Psi_D^n = \tilde{\Psi}^{n+1} - \Psi^{n-1} = D_\Psi^n \ 2\ \Delta t \ , \qquad (3)$$

where $\tilde{\Psi}^{n+1}$ is a provisional value at $t=(n+1)\Delta t$ i.e. the value that is found with dynamics only. The scheme is three time level, explicit and second order accurate. Ideally, one would use the same scheme for the parametrized part of the equations as well. With such an explicit scheme it is irrelevant whether different terms are evaluated separately or as a single forcing; the increments due to different terms are independent.

Unfortunately the leapfrog scheme can not be used for the parametrized processes because most of these processes are diffusive in nature and the leapfrog scheme is unconditionally unstable for parabolic equations. Therefore for the tendencies of some of the parametrized processes a forward time scheme is used (e.g. radiation), for others an implicit (backward) time scheme is used (e.g. vertical diffusion). The two examples give increments according to

$$\Delta\Psi_R^n = \tilde{\Psi}^{n+1} - \Psi^{n-1} = R_\Psi^{n-1} \ 2\ \Delta t \ , \qquad (4)$$

for radiation and

$$\Delta\Psi_{VD}^n = \tilde{\Psi}^{n+1} - \Psi^{n-1} = VD^{n+1} \ 2\ \Delta t \ , \qquad (5)$$

for vertical diffusion, where VD is evaluated with $\tilde{\Psi}^{n+1}$ i.e. Ψ^{n-1} incremented with the vertical diffusion contribution only. Fractional steps instead of process splitting applied to vertical diffusion would change equation (5) in

$$\Delta\Psi_{VD}^{n} = \tilde{\Psi}^{n+1} - \{\Psi^{n-1} + \Delta\Psi_{D} + \Delta\Psi_{R}\} = VD^{n+1}\ 2\ \Delta t\ . \qquad (5a)$$

The choice of schemes as described above has important implications for the accuracy of the time stepping. Unlike the scheme for the dynamics, the time integration of the sub-grid processes is first order accurate only. Furthermore, the effective time step is $2\Delta t$, twice the value one would have with a normal two level forward integration with the same number of time steps. The reason is that the leapfrogging in the dynamics imposes a $2\Delta t$ integration interval every time step and that midpoint evaluation of the tendencies is not possible for the parametrized processes because of stability limitations.

Given the fact that a number of sub-grid processes have short time scales compared to the time step, it is probably difficult to develop a stable second order time stepping scheme. On the other hand it is not very satisfactory to lose accuracy with double time steps by doing the same time path twice with a first order scheme. A solution would be to divide the $2\Delta t$ increment in two increments with one Δt interval for the sub-grid processes. So we define the increment for the parametrized physics for one Δt as

$$\Delta\Psi_{P}^{n+1/2} = \tilde{\Psi}^{n+1} - \Psi^{n} = P_{\Psi}^{n}\ \Delta t\ , \qquad (6)$$

and find the increment for a double time step by adding the increments for two single time steps. The expression for Ψ^{n+1} is

$$\Psi^{n+1} - \Psi^{n-1} = \Delta\Psi_{D}^{n} + \Delta\Psi_{P}^{n-1/2} + \Delta\Psi_{P}^{n+1/2}\ . \qquad (7)$$

From the point of view of processing time, equation (7) is not more expensive than the double time step scheme. The disadvantage of equation (7) is that the increments have to be stored for one time step. In the framework of the ECMWF model this would mean that the grid point work files need 4 extra three dimensional grid point fields to carry the increments of the parametrized physics from one time step to the next. To limit the size of the work files, the ECMWF model integrates the sub-grid processes over $2\Delta t$ instead of using equation (7). This may be something to reconsider when work files limitations become less restrictive. Development of the new time stepping scheme for the adiabatic equations (two time level semi- Lagrangian), which is envisaged for

the ECMWF model, will alleviate this problem as well.

We now describe the numerical aspects of the different processes in the order they are dealt within the model.

2.1 Radiation

The radiation tendency can be expressed as a radiative flux divergence:

$$\frac{\partial T}{\partial t} = \frac{g}{C_p}\frac{dF}{dp} \tag{8}$$

where g is the gravitational acceleration, C_p the specific heat at constant pressure, F the radiative flux and p the pressure. The radiation scheme computes the radiative fluxes at half levels from the moisture and temperature profile at time step (n-1). The temperature increment for level j due to radiation is now derived from simple finite differencing in the vertical

$$(\Delta T_j)_R = 2\Delta t \ \frac{g}{C_p}\ \frac{F^{n-1}_{j+1/2} - F^{n-1}_{j-1/2}}{p_{j+1/2} - p_{j-1/2}} \tag{9}$$

The index j refers to the full model levels and j+1/2 and j-1/2 to the half levels (see Fig. 1). The half levels are prescribed and the full levels are in the middle between the half levels. The model variables U, V, T and q are defined on the full levels. By having the fluxes staggered with respect to the levels where T is defined, internal energy is automatically conserved.

The radiation is probably the simplest of the parametrized processes with regard to numerical stability and accuracy as the radiative fluxes rather act as a nearly constant forcing than as a diffusive process. In clear sky situations the radiative fluxes depend only weakly on the temperature and moisture profiles; the fluxes are much more determined by the net fluxes at the lower and upper boundary of the atmosphere. The clear sky radiative flux divergence over the entire atmosphere is of the order of 100 W/m^2, which gives us a time scale of the order of 10 days for a temperature change of 10 K. This long time scale compared to the time step of the model (Δt = 15 minutes at T106) makes it possible to use an explicit scheme without running into stability problems. To save time in the rather expensive radiation computations, the full radiation code is called every 3 hours only to evaluate the emissivities and absorption coefficients. The fluxes are adjusted every time step to account for the change in solar angle.

The behaviour of the radiation becomes more radical when cloud layers develop, particularly at low levels. A stratocumulus layer can generate a flux divergence of nearly 100 W/m^2 over a sharp interface. The model can not resolve such interfaces but will smear the divergence over one model layer of e.g. 20 hPa when it occurs very close to the surface. The resulting cooling of this layer is about 2 K per hour or 1 K increment for a single radiation step over $2\Delta t$. The real atmosphere is probably very close to a steady state because other processes compensate for the strongly localized radiative cooling. It is clear from this example that the kind of situations where large compensating tendencies occur in different processes is extremely sensitive to time truncation errors. We will discuss this problem in more detail in section 3.

2.2 Vertical diffusion

Vertical diffusion is formulated in terms of dry static energy, specific humidity, and the two horizontal wind components. The tendency due to subgrid turbulence is

$$\frac{\partial \Psi}{\partial t} = g \frac{dF_\Psi}{dp} \tag{10}$$

where F_Ψ is the turbulent flux parametrized as

$$F_\Psi = K_\Psi \rho \frac{d\Psi}{dz} \tag{11}$$

and K_Ψ is the exchange coefficient for quantity Ψ and ρ air density. The finite difference scheme reads

$$(\Delta\Psi_j)_{VD} = \tilde{\Psi}_j^{n+1} - \Psi_j^{n-1} =$$

$$\frac{2\Delta t\, g}{p_{j+1/2} - p_{j-1/2}} \left[- K_{j+1/2}^{n-1} \frac{\tilde{\Psi}_{j+1}^{n+1} - \tilde{\Psi}_j^{n+1}}{z_{j+1} - z_j} + K_{j-1/2}^{n-1} \frac{\tilde{\Psi}_j^{n+1} - \tilde{\Psi}_{j-1}^{n+1}}{z_j - z_{j-1}} \right], \tag{12}$$

$$\tilde{\Psi}^{n+1} = \alpha\, \tilde{\Psi}^{n+1} + (1-\alpha)\, \Psi^{n-1}.$$

Parameter α determines the implicitness of the scheme; for $\alpha=0$ the scheme is

explicit, for α=0.5 we have the Crank Nicholson scheme and for α=1 we have the implicit backward scheme. In the operational ECMWF model α=1.5 to avoid non-linear instability from the K-coefficients. The exchange coefficients depend on the local wind shear and on the local stability expressed by a Richardson number dependence; they are evaluated at time level n-1. The resulting algebraic set of equations forms a tridiagonal matrix which can be solved very efficiently.

2.3 Gravity wave drag

From the numerical point of view gravity wave drag is very similar to the vertical diffusion and requires an implicit treatment for stability reasons. The implicitness factor α is 1. In practice the gravity wave scheme is a little less critical from the stability point of view than the vertical diffusion scheme probably because it is more linear and only locally active.

2.4 Deep and shallow convection

Deep and shallow convection are currently parametrized by a mass flux scheme, in which the vertical transport is assumed to take place in up- and downdrafts which occupy only a small fraction of the grid square and by induced subsidence in the remaining fraction of the grid square (Tiedtke 1989):

$$\frac{\partial \Psi}{\partial t} = g \frac{d}{dp} \left[M_u \Psi_u + M_d \Psi_d - (M_u + M_d) \Psi \right] + S \ , \qquad (13)$$

where M_u and M_d are the upward and downward mass fluxes respectively, $\Psi_{u,v}$ are the values of Ψ (U, V, s and q) in the up and down drafts, and S is a source term for the equations of dry static energy and specific humidity, representing: condensation/sublimation, evaporation of cloud water detrained into the the unsaturated environment and evaporation of rain/snow and melting of snow. If we assume that the parametrization scheme prescribes $M_{u,v}$ and $\Psi_{u,v}$, the time stepping scheme is as follows:

$$(\Delta\Psi_j)_C = \tilde{\Psi}_j^{n+1} - \left\{\Psi_j^{n-1} + (\Delta\Psi_j)_D + (\Delta\Psi_j)_{RD} + (\Delta\Psi_j)_{VD} + (\Delta\Psi_j)_{GWD}\right\} =$$

$$\frac{2\Delta t\, g}{p_{j+1/2} - p_{j-1/2}}\Big[(M_u\Psi_u + M_d\Psi_d)_{j+1/2} - (M_u\Psi_u + M_d\Psi_d)_{j-1/2}$$

$$(M_u + M_d)_{j+1/2}\Psi_j - (M_u + M_d)_{j-1/2}\Psi_{j-1}\Big] + S_j \qquad (14)$$

There are a few things to note here:

- Central differences are used in the vertical to specify flux divergence, but the values of M_u, M_d and Ψ_u, Ψ_d are calculated using upstream methods. The mass flux M_u+M_d acts as downward advection and causes instabilities when central differencing is used. Therefore upwind differencing is applied.
- The scheme is conservative because successive levels share the same fluxes at half levels.
- The closure which prescribes the cloud base mass flux is constructed in such a way that the moisture profile below cloud base remains unchanged, i.e. a balance between moisture convergence, surface fluxes and convection tendencies below cloud base. To ensure that a quasi-steady state is generated, the tendencies of some other processes are passed to the mass flux parametrization. In the ECMWF model the convection scheme starts from the profiles at (t-1) incremented with radiation, vertical diffusion and gravity wave effects. This can be interpreted as a method of fractional steps.
- Input for convective calculations must (i) not be supersaturated (otherwise adjustment as for large scale precipitation) and (ii) be dry convectively stable as vertical advection would destabilize the atmosphere further.
- The mass flux is limited according the stability criterion: $M_u < \rho\Delta z/2\Delta t$.
- It has proved to be necessary with longer time steps in the high resolution model (T213L31) to modify equation (14) for the momentum components to a partially implicit scheme whereby updated values of Ψ are used wherever possible as the column values are solved from top to bottom.

2.5 Large scale precipitation

The large scale precipitation is parametrized as an instantaneous adjustment that removes all moisture above 100 % relative humidity. If for the specified specific humidity and temperature super saturation occurs, the temperature and moisture are adjusted such that the relative humidity is 100 % and that internal energy is conserved. It is essential that the output fields of T and q are realistic, and are not supersaturated. Therefore the T and q adjustment is done as the last process after all increments have been added to the variables at time level n-1. So we start from

$$\tilde{T}_j = T_j^{n-1} + (\Delta T^n)_D + (\Delta T^n)_R + (\Delta T^n)_{VD} + (\Delta T^n)_C \tag{15}$$

$$\tilde{q}_j = q_j^{n-1} + (\Delta T^n)_D + (\Delta q^n)_R + (\Delta q^n)_{VD} + (\Delta q^n)_C \tag{16}$$

The adjustment to the new values T^{n+1} and q^{n+1} is such that

$$q_j^{n+1} = q_{sat}(T_j^{n+1}) \quad \text{and} \tag{17}$$

$$\tilde{q}_j - q_j^{n+1} = (C_p/L)\,(T_j^{n+1} - \tilde{T}_j), \tag{18}$$

where L is the latent heat of vaporization. This set of equations is solved by linearizing the saturated specific humidity function

$$(\Delta T_j^n)_{LSP} = \left\{(\tilde{q}_j - q_{sat}(\tilde{T}_j)\right\} \left\{ \frac{C_p}{L} + \frac{dq_{sat}}{dT} \right\}^{-1} \tag{19}$$

$$(\Delta q_j^n)_{LSP} = - (\Delta T_j^n)_{LSP} \; (C_p/L) \tag{20}$$

3. THE ORDER OF THE PROCESSES IN THE TIME INTEGRATION

From the overview in section 2 it has become clear that the order of the processes in the process splitting is relevant. The reason for having to use implicit schemes is that we apply a relatively long time step to a process with a short time scale. In the extreme case of a process that leads to an instantaneous adjustment, it means that the implicit scheme brings the profiles into equilibrium, but without taking the other tendencies into account it can be the wrong equilibrium. Examples are:

- The vertical diffusion of momentum tends to come into equilibrium with the Coriolis term and the pressure gradient term to generate the well known Ekman profile. Without having the dynamic tendencies in the implicit computation of the diffusion, the diffusion scheme will relax towards the wrong equilibrium for long time steps.
- The stratocumulus topped boundary layer cools from the top and the cooling is concentrated in a very shallow layer. In discretized form the cooling will be in a single layer. The vertical diffusion redistributes this cooling over the mixed layer almost instantaneously. Without feeding the radiative tendencies into the vertical diffusion scheme, the profiles cannot adjust and noisy profiles will be generated for long time steps.

In general it can be stated that the time evolution of the fields is much slower than due to a single physical process only, i.e. when tendencies for a single process are large, they are often compensated by other processes. With large time steps it is therefore important to balance the different processes within one time step. In principle one would have to order the processes according to their time scale, the slow processes first (explicit time integration) and after that the fast processes (implicit) acting on the fields that are already incremented by the other processes. With more than one implicit process there is no real solution to the ordering problem. It may be beneficial to compute the tendencies of some processes twice, just to ensure that all the processes come into equilibrium within one time step.

4. RECENT DEVELOPMENTS WITH VERTICAL DIFFUSION

4.1 Vertical resolution

To investigate the effect of vertical resolution on the boundary layer structure that is produced by the model we integrate the simple Ekman equations over a 9 hour interval with different boundary conditions for the heat flux at the surface to generate typical day and night time boundary layers. The idea is that after a few hours with constant forcing, the boundary layer reaches a quasi-steady state. The remaining time evolution, which is the result of inertial oscillation, is weak and cancels out when two similar runs are compared. The Ekman equations are

$$\frac{\partial U}{\partial t} = -f(V-V_G) + g\frac{\partial F_U}{\partial p}, \qquad F_U = -K_M \rho \frac{\partial U}{\partial z} , \tag{21}$$

$$\frac{\partial V}{\partial t} = f(U-U_G) + g\frac{\partial F_V}{\partial p}, \qquad F_V = -K_M \rho \frac{\partial V}{\partial z} , \tag{22}$$

$$\frac{\partial \theta}{\partial t} = + g\frac{\partial F_\theta}{\partial p}, \qquad F_\theta = -K_H \rho \frac{\partial \theta}{\partial z} , \tag{23}$$

where K_M and K_H are the exchange coefficients for momentum and heat as specified by the parametrization (see Louis 1979 and Louis et al., 1982), f is the Coriolis parameter ($10^{-4}s^{-1}$ for these model experiments) and θ is the potential temperature. The vertical discretization makes use of model variables at full levels and fluxes at half levels (see Fig. 1).

The increments from one double time step are evaluated in the following way

$$U_j^{n+1} - U_j^{n-1} = 2\Delta t\left\{ g\frac{F_{Uj+1/2} - F_{Uj-1/2}}{p_{j+1/2} - p_{j-1/2}} + f(V^{n-1} - V_G)\right\} , \tag{24}$$

$$V_j^{n+1} - V_j^{n-1} = 2\Delta t\left\{ g\frac{F_{Vj+1/2} - F_{Vj-1/2}}{p_{j+1/2} - p_{j-1/2}} - f(U^{n-1} - U_G)\right\} , \tag{25}$$

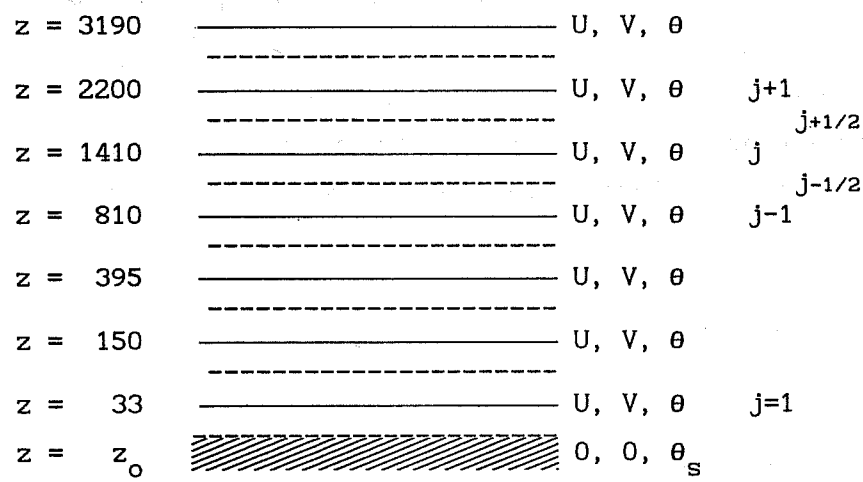

Fig. 1 The vertical grid structure near the surface in the ECMWF 19-level model.

$$\theta_j^{n+1} - \theta_j^{n-1} = 2\Delta t\ g\ \frac{F_{\theta j+1/2} - F_{\theta j-1/2}}{p_{j+1/2} - p_{j-1/2}}\ , \tag{26}$$

$$\tilde{\Psi}^{n+1} = \alpha\ \tilde{\Psi}^{n+1} + (1-\alpha)\ \Psi^{n-1}, \quad \text{where } \Psi = U,V \text{ or } \theta, \tag{27}$$

$$F_{\Psi j+1/2} = -K^{n-1}_{\Psi j+1/2}\ \frac{\tilde{\Psi}^{n+1}_{j+1} - \tilde{\Psi}^{n+1}_{j}}{z_{j+1} - z_j}\ . \tag{28}$$

Note that in this stand alone version of the vertical diffusion code the leapfrog scheme has been replaced by an explicit forward scheme for the Coriolis term. The time integration step is defined as $2\Delta t$ for comparison with the operational ECMWF model. The centered difference approximation for the fluxes is applied to all model levels except in the surface layer, where a linear approximation of the profiles would be too inaccurate. The finite difference formulation of the fluxes in the surface layer relies on

$$F_\Psi = -\rho\ K_\Psi\ \frac{\partial \Psi}{\partial z}\ , \tag{29}$$

integrated analytically between the surface and the height of the lowest model level, assuming that F_Ψ is constant and accounting for the specific z-dependence in K_Ψ (proportional to z in the neutral case). Instead of equation (28) we have now the surface layer similarity profiles (logarithmic form plus stability correction)

$$F_\Psi = -\rho\ k\ u_*\ (\Psi_1 - \Psi_s)\ \left(\ln\left(\frac{z_1}{z_o}\right) - F_\Psi\left(\frac{z_1}{L}\right) \right)^{-1}, \tag{30}$$

where u_* is the friction velocity, F_Ψ the stability correction function and L the Obukhov length. This expression can be seen as a finite difference formulation of the surface layer. The equivalent form of (28) is

$$F_{\Psi 1/2} = -C\ (\tilde{\Psi}^{n+1}_1 - \tilde{\Psi}^{n+1}_s)\ , \tag{31}$$

where $C = \rho\, k\, u_* \left(\ln(\frac{z_1}{z_o}) - F_\Psi(\frac{z_1}{L}) \right)^{-1}$, evaluated at n-1.

The interesting aspect of finite difference form (31) is that it is exact provided that the fluxes are constant between the surface and the lowest model layer in spite of the logarithmic singularity in the wind and temperature profiles. The accuracy of the constant flux approximation for the surface layer can be assessed by considering that the flux has a nearly linear height dependency varying from the surface value to zero at the top of the boundary layer. The boundary layer height is of the order of 1000 m for the unstable boundary layer (day time over land) and of the order 100 m for the stable boundary layer. With the lowest model level at 32 m (ECMWF 19-level model), the constant flux approximation is fairly accurate for the unstable boundary layer, but can be questioned for the stable boundary layer.

Because the stable boundary layer is shallow and therefore most likely to show discretization errors, we compare two integrations: one with the operational 19-level resolution and one with a much higher resolution (the distribution of layers can be seen from the figures). A constant downward surface heat flux of 20 W/m^2 is imposed as boundary condition. Because the ECMWF closure scheme (Louis et al. 1982) tends to overestimate the depth of the stable boundary layer, the results of an alternative scheme (Beljaars and Holtslag, 1991) are also shown. The stress profiles and the wind profiles are shown in the Figs. 2 and 3 for the two closure schemes. The effect of the resolution is relatively small. Even the extremely shallow stable boundary layer of Fig. 3 is fairly well reproduced. This is quite remarkable since the boundary layer is resolved by two or three levels only. The high performance of the scheme is partially due to the use of an exact surface layer formulation as finite difference between the surface and the lowest model level. Another effect was recently pointed out by Delage (1988). He shows that neglecting flux divergence in the surface layer compensates for neglecting the effect of the asymptotic mixing length in the surface layer.

To investigate the effect of vertical resolution over the entire stability range, 9-hour integrations have been made with different surface heat fluxes and a constant geostrophic wind of 10 m/s. The friction velocity and the ageostrophic angle of the surface wind are plotted in Fig. 4.

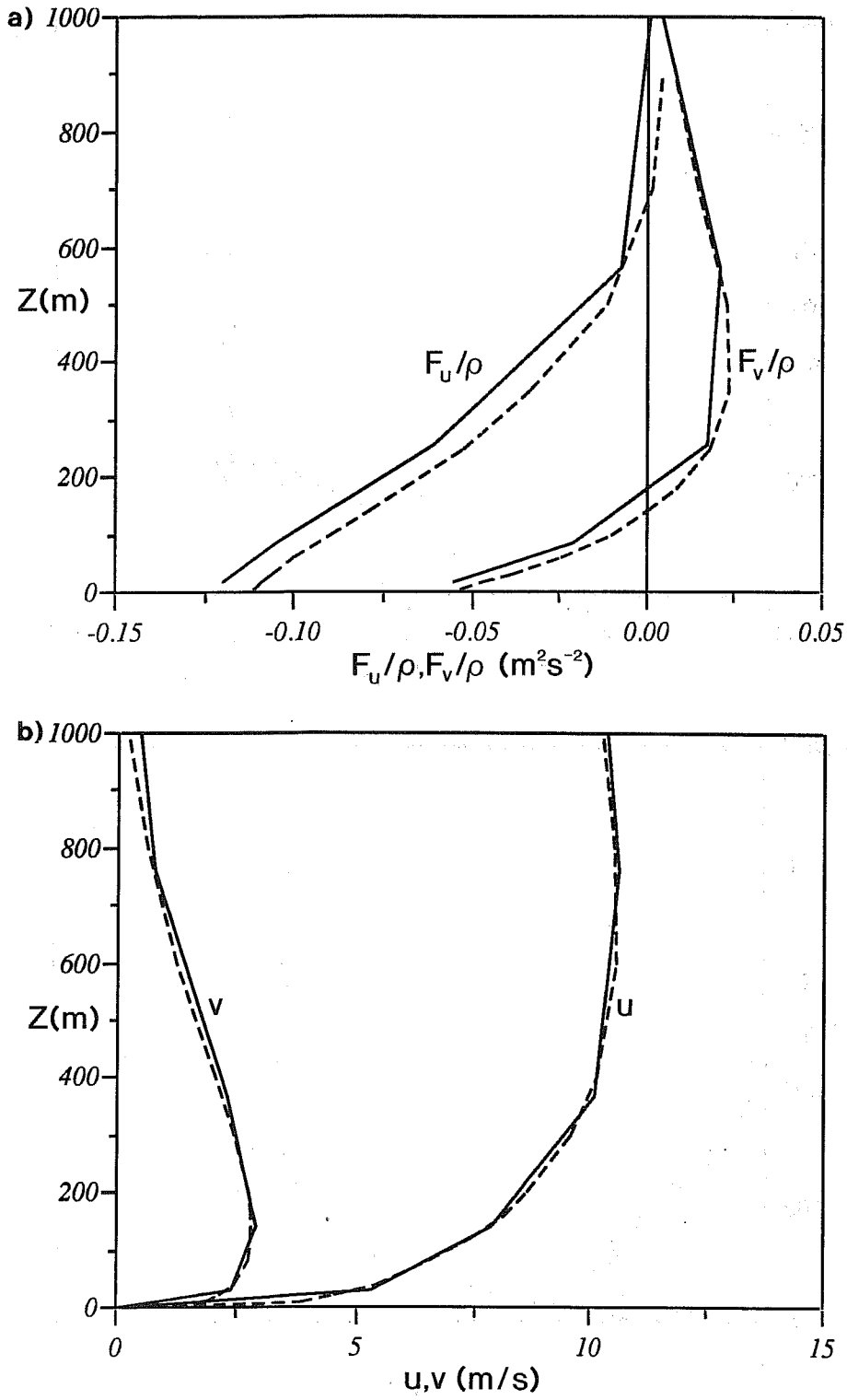

Fig. 2 Stress profiles (a) and wind profiles (b) after 9 hours of integration of the Ekman equations with a constant heat flux of 20 W/m^2. The ECMWF operational closure scheme is used (Louis et al., 1982) combined with high resolution (dashed) and the ECMWF 19-level resolution (solid).

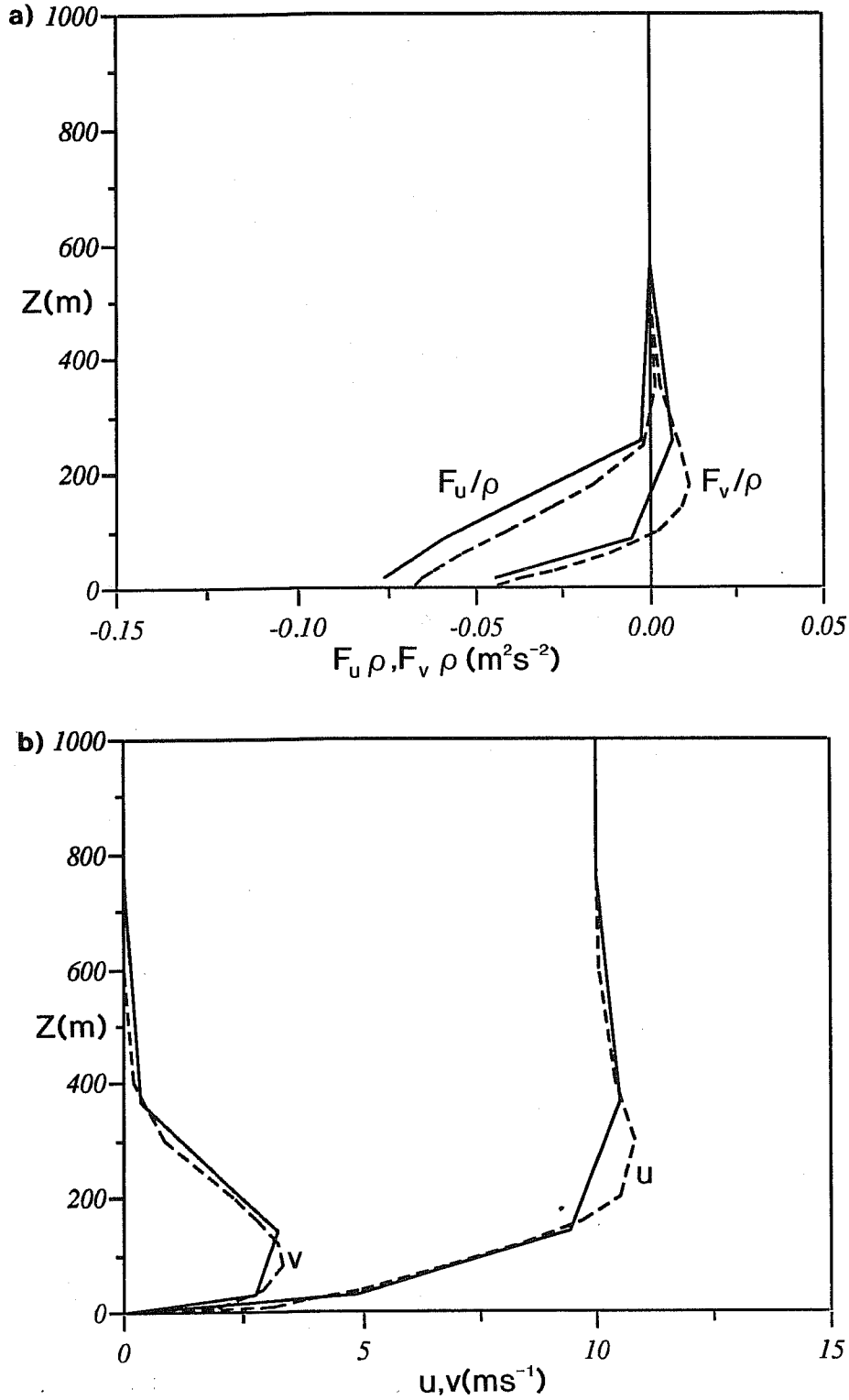

Fig. 3 Stress profiles (a) and wind profiles (b) after 9 hours of integration of the Ekman equations with a constant heatflux of 20 W/m^2. Closure according to Beljaars and Holtslag (1991) combined with high resolution (dashed) and the ECMWF 19-level resolution (solid).

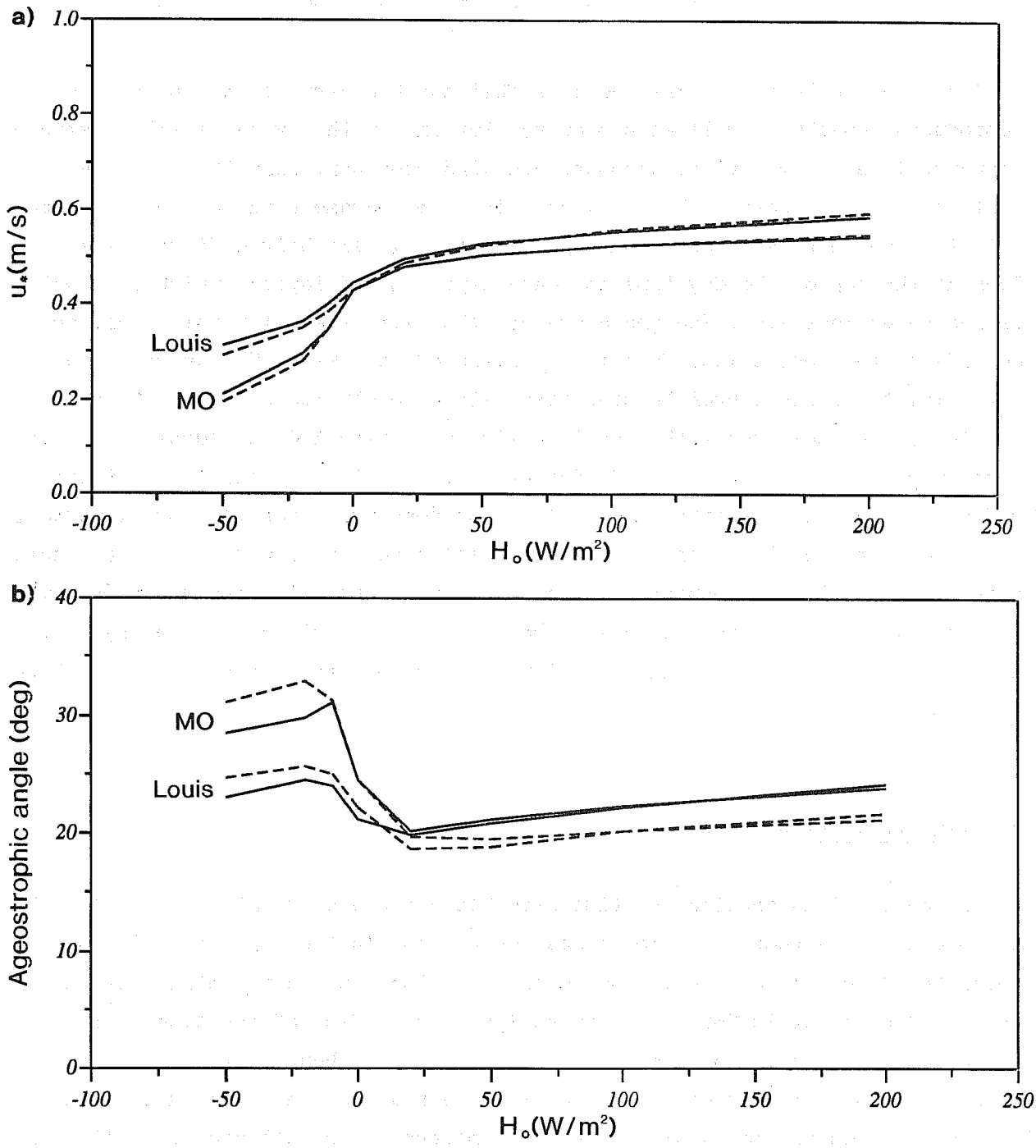

Fig. 4 Friction velocity (a) and ageostrophic angle (b) as function of heat flux at the surface after 9 hours of integration of the Ekman equations. Two closure schemes are applied (closure A: Louis et al., 1982; closure B: Beljaars and Holtslag, 1991) combined with high resolution (dashed) and the ECMWF 19-level resolution (solid).

The main conclusion we draw here is that the boundary layer structure is reproduced remarkably well with poor resolution. In the very shallow stable boundary layer, some of the ageostrophic wind component near the surface is lost, as to be expected, but changes in the parametrization have larger effects than improved resolution. The situation is slightly different when we look at the top of the day time boundary layer (mixed layer), which is usually capped by an inversion. The sharpness of the simulated inversion obviously depends on the resolution. This is illustrated in Fig. 5, which shows a potential temperature profile simulated with a resolution of about 600 m near the inversion, compared with a profile simulated with 200 m resolution. The temperature profiles are quite different, although the vertically integrated difference equals zero (the numerical scheme conserves energy). How important it is to represent the capping inversion realistically is not clear at this moment. It is to be expected however, that vertical resolution becomes increasingly relevant in the case of boundary layer clouds. Boundary layer clouds are shallow (a few hundreds of meters deep) and capped by a sharp inversion.

4.2 Time truncation

In the previous section the time step $2\Delta t$ was chosen relatively small (450 s) to minimize effects of time truncation errors. In the operational T106L19 model the double time step is 1800 s and in the low horizontal resolution model (T42L19) $2\Delta t$ is 3600 s. To investigate the effect of the time step, the one column version of the model is integrated over 9 hours with different time steps and two different methods. The first method is the one described in section 4.1, where the dynamic terms are integrated simultaneously with the diffusion terms. We will call it the "method of fractional steps" because equation (25) and (26) can be applied in two steps: (i) increase the n-1 winds with the dynamic terms and then (ii) apply the vertical diffusion from the provisional profiles (however, the K-coefficients are still evaluated at n-1). The second method uses "process splitting", it does not contain the terms $2\Delta tf(U-U_G)$ and $2\Delta tf(V-V_G)$ in equation (25) and (26) but adds these terms separately to find the full increment of one time step. The geostrophic wind

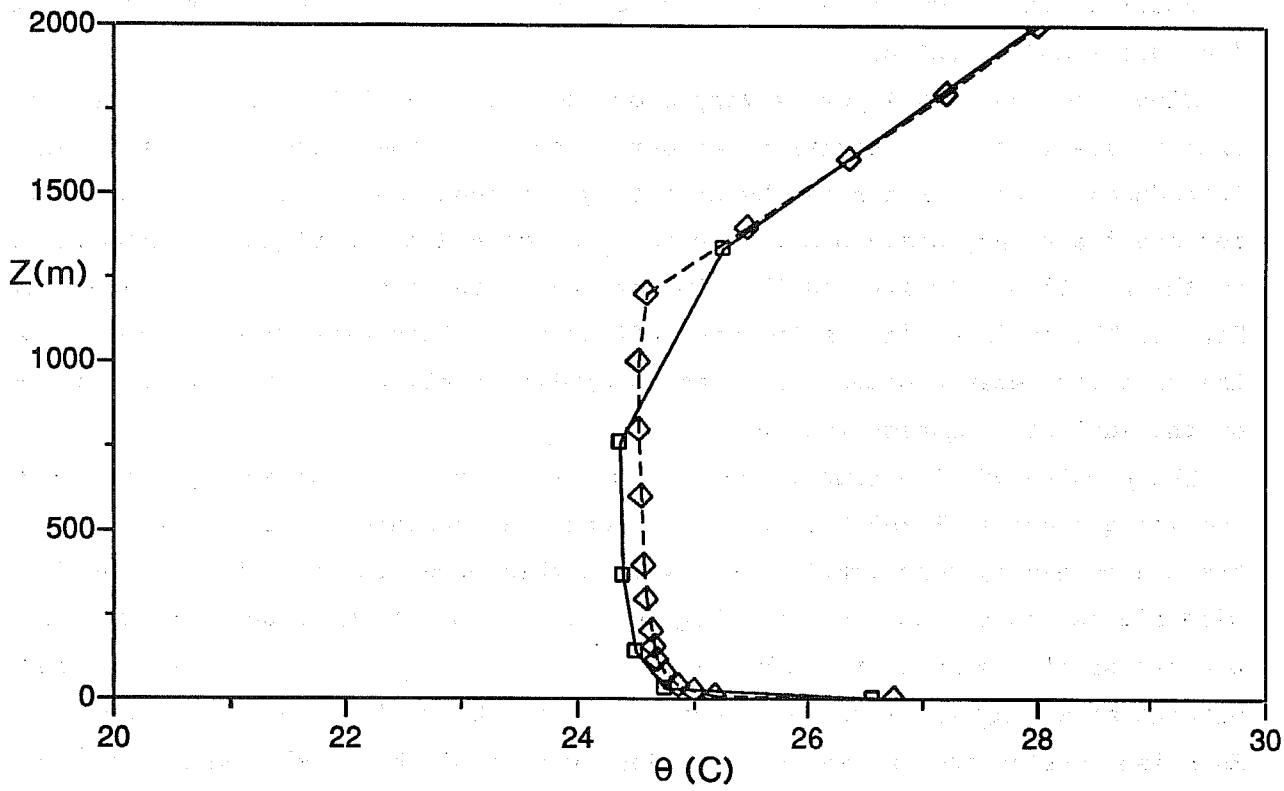

Fig. 5 Potential temperature profile after 9 hours of integration of the Ekman equations with a constant heat flux of 100 W/m^2. High resolution (dashed) and the ECMWF 19-level resolution (solid) are used.

is set to a constant value of 10 m/s in the x-direction and neutral stratification is considered only. Three different roughness lengths are used: 1 m, 0.1 m and 0.0001 m.

Since the boundary layer is very close to a steady state after 9 hours, we expect small time truncation errors. However, the "process splitting" introduces truncation errors; by splitting the equations into two parts we replace the steady state problem by two time dependent problems. A comparison of the friction velocity and the wind at the lowest model level is given in Fig. 6. The surface wind is the most affected; it increases with the length of the time step when process splitting is applied particularly for high values of the surface roughness length.

The problem of time truncation errors was recently raised by the wave modelling group at ECMWF because they found that surface stress fields over the oceans had systematically lower values than expected from the near surface wind fields. As can be seen from Fig. 6, the time truncation errors (with process splitting as in the ECMWF model) result in increased surface winds without affecting the surface stress very much. Only with the very recent U,V Eulerian version and the semi-Lagrangian version of the ECMWF model it has been possible to apply the method of fractional steps. The previous vorticity and divergence formulation did not have the full dynamic tendencies in grid-point space. To investigate the effect of the time step length, the global ECMWF model has been integrated over a 6 hour interval with $2\Delta t$ equal to 120 s and 1800 s (time step for the operational T106L19 model) and two schemes: process splitting and fractional steps. The experiments with 120 s can be used as a reference because they have very small time truncation errors and the difference between the two schemes (not shown) turns out to be extremely small. After six hours the large scale fields are still very similar and the boundary layer has come into equilibrium with the dynamic forcing after a short time.

The time truncation errors of the wind vectors (1800 s minus 120 s integration) at the lowest model level are shown as relative errors in the Figs. 7 and 8 for the process splitting scheme and the fractional step method respectively. The relative vectors have been calculated by taking the vector difference and rotating the reference vector Northward and scaling it to 100%. A Nortward pointing relative error vector means that the error results in too

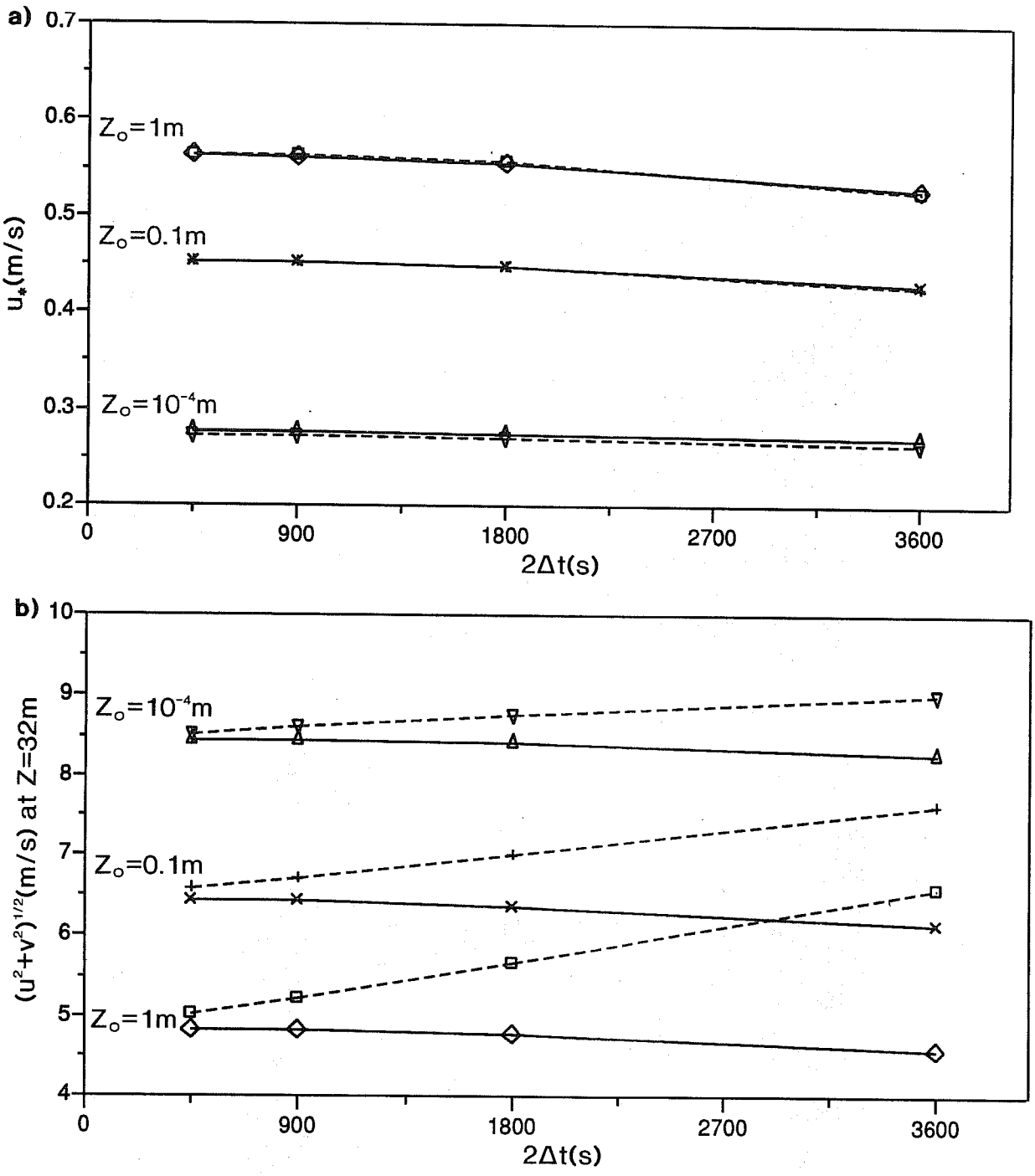

Fig. 6 Friction velocity (a) and wind at lowest model level 32 m; (b) as function of time step after 9 hours of integration with zero heat flux at the surface. Two schemes are applied: the process splitting scheme (dashed) and method of fractional steps (solid).

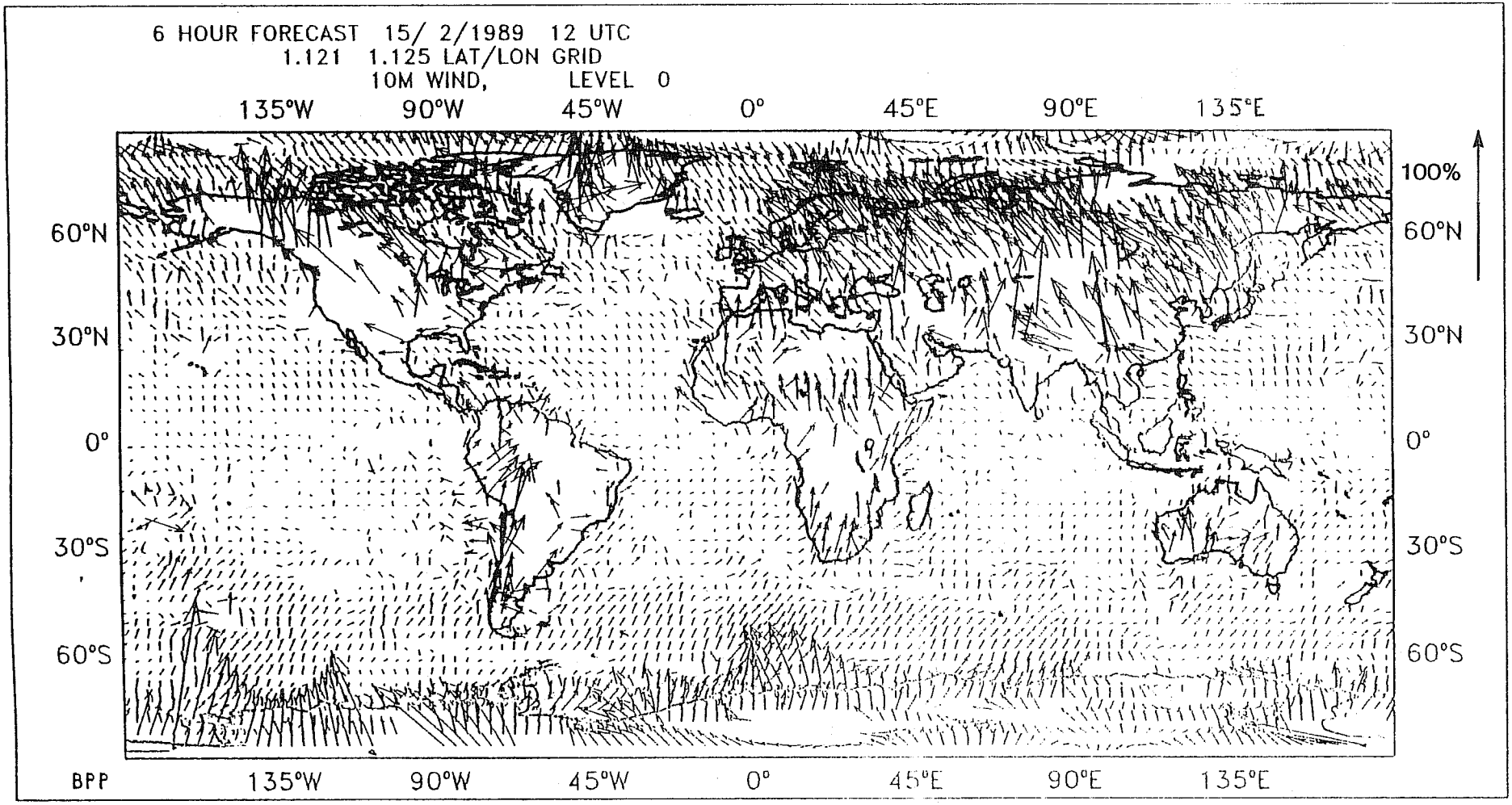

Fig. 7 Relative wind errors at the lowest model level due to time truncation for the integration with process splitting. The error vectors are computed by taking the difference between the 1800 s time step integration and the reference integration ($2\Delta t$=120 s) after rotating and scaling the vectors until the reference vector points North and has a length of 100 %.

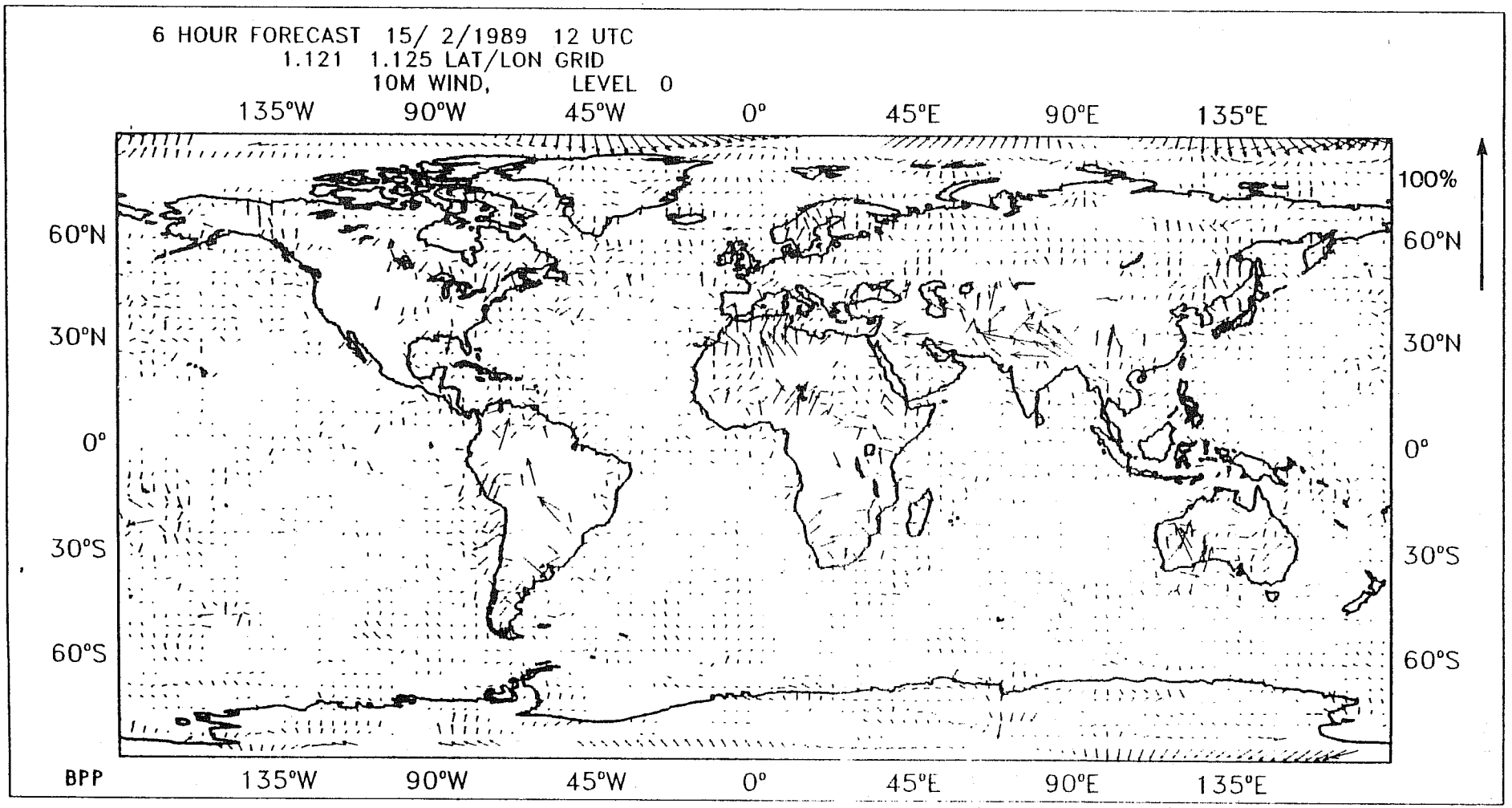

Fig. 8 Relative wind errors with the method of fractional steps (see also caption of Fig. 7)

large wind speeds; the Westward tilt over the Northern Hemisphere and the East tilt over the Southern hemisphere mean that the ageostrophic angle is too large (boundary layer wind veers with height at the Northern hemisphere and backs with height at the Southern hemisphere). Errors in the surface stress are shown in Fig. 9 and 10 for the two schemes. These results are consistent with the one dimensional experiments, although we find a great deal of scatter which is probably related to time dependencies in the real atmosphere.

The inconsistency between surface winds and surface stresses is most clearly shown by the scatter plots of the drag coefficient for the Southern Hemisphere over ocean (Fig. 11). The solid line indicates the drag coefficient that is imposed by the parametrization according to the Charnock relation and the individual points have been derived from model winds and stresses at grid points over sea. We see that systematic errors occur with the process splitting, particularly at large wind speeds. The method of fractional steps eliminates the systematic error and slightly reduces the scatter.

4.3 Stability

The vertical diffusion introduces relatively short time scales in the model and it is therefore not a surprise that an implicit treatment is necessary for stability reasons. The problem is even more complicated because the diffusion coefficients are a function of the local wind shear and the local Richardson number. For simplicity the diffusion coefficients are usually evaluated explicitly (for time level n-1; see equation 28). This can introduce a non-linear instability particularly in stable situations when the exchange coefficients vary strongly with the Richardson number.

Girard and Delage (1990) address the stability aspects of the numerical solution of the coupled set of one dimensional diffusion equations with fairly realistic exchange coefficients.

$$\frac{\partial U}{\partial t} = \frac{\partial}{\partial z} K_M \frac{\partial U}{\partial z}, \qquad \frac{\partial \theta}{\partial t} = \frac{\partial}{\partial z} K_H \frac{\partial \theta}{\partial z}. \tag{32}$$

As closure they use

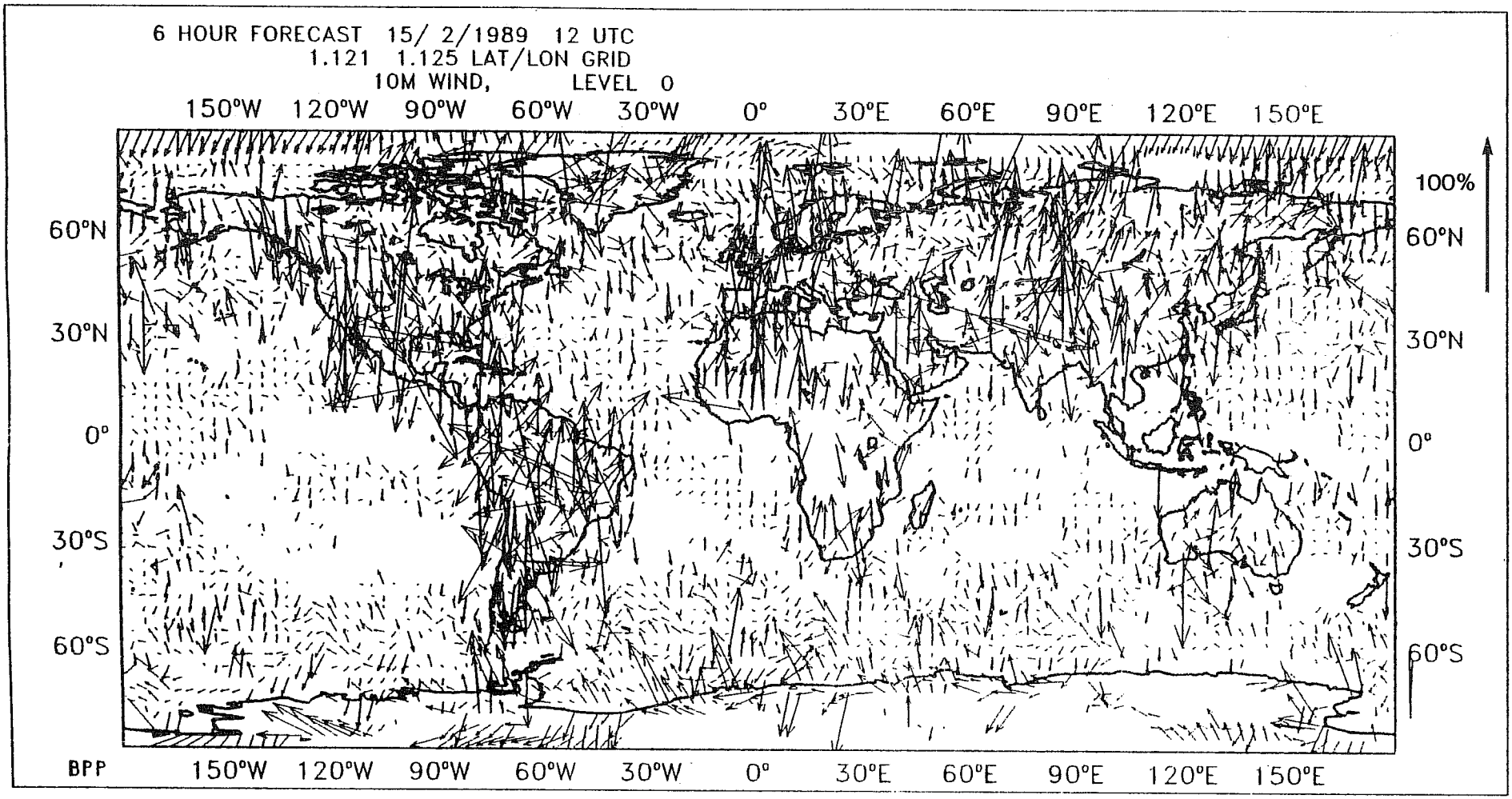

Fig. 9 Relative surface stress errors with process splitting (see also caption of Fig. 7)

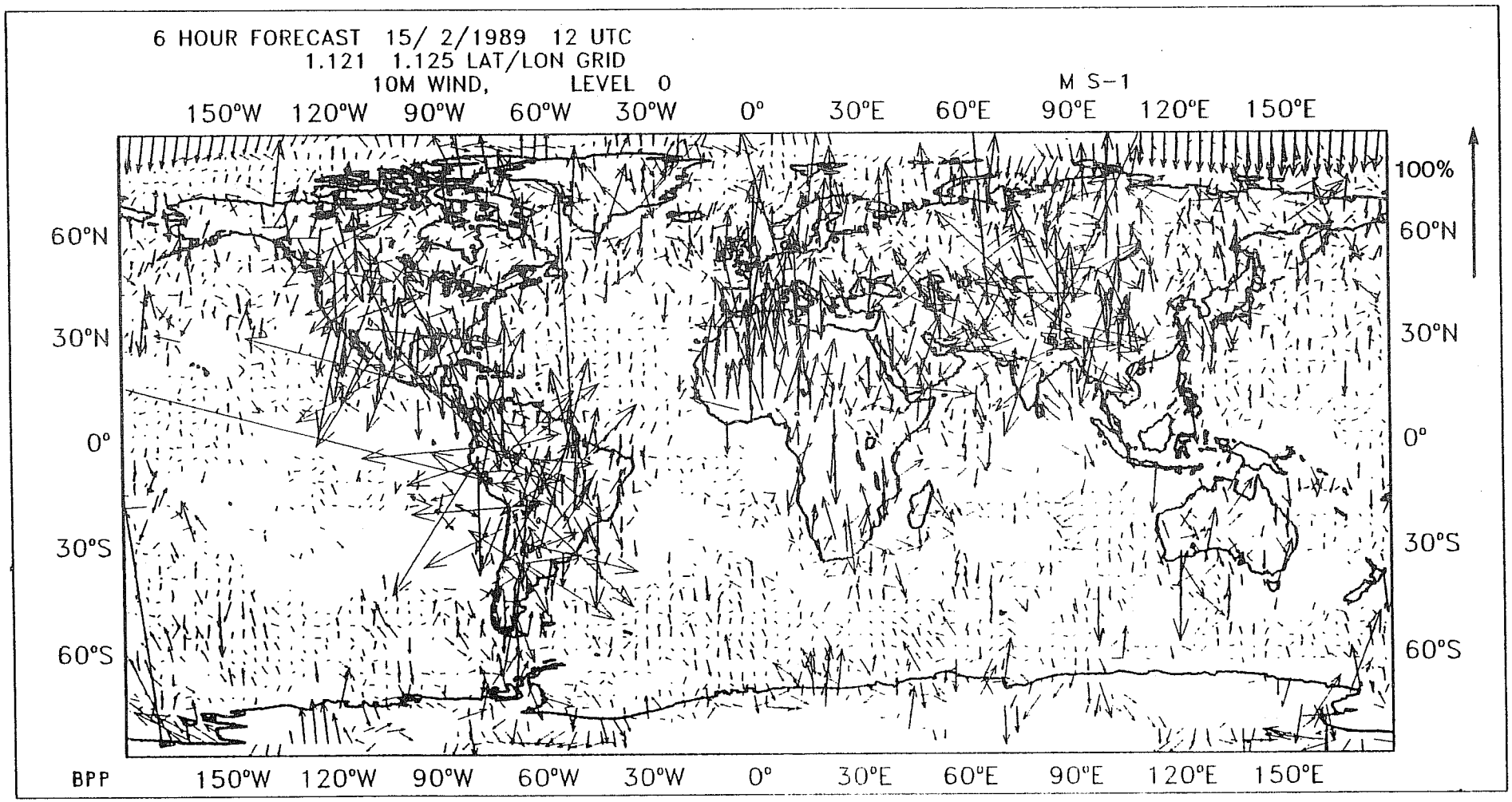

Fig. 10 Relative surface stress errors with method of fractional steps (see also caption of Fig. 7)

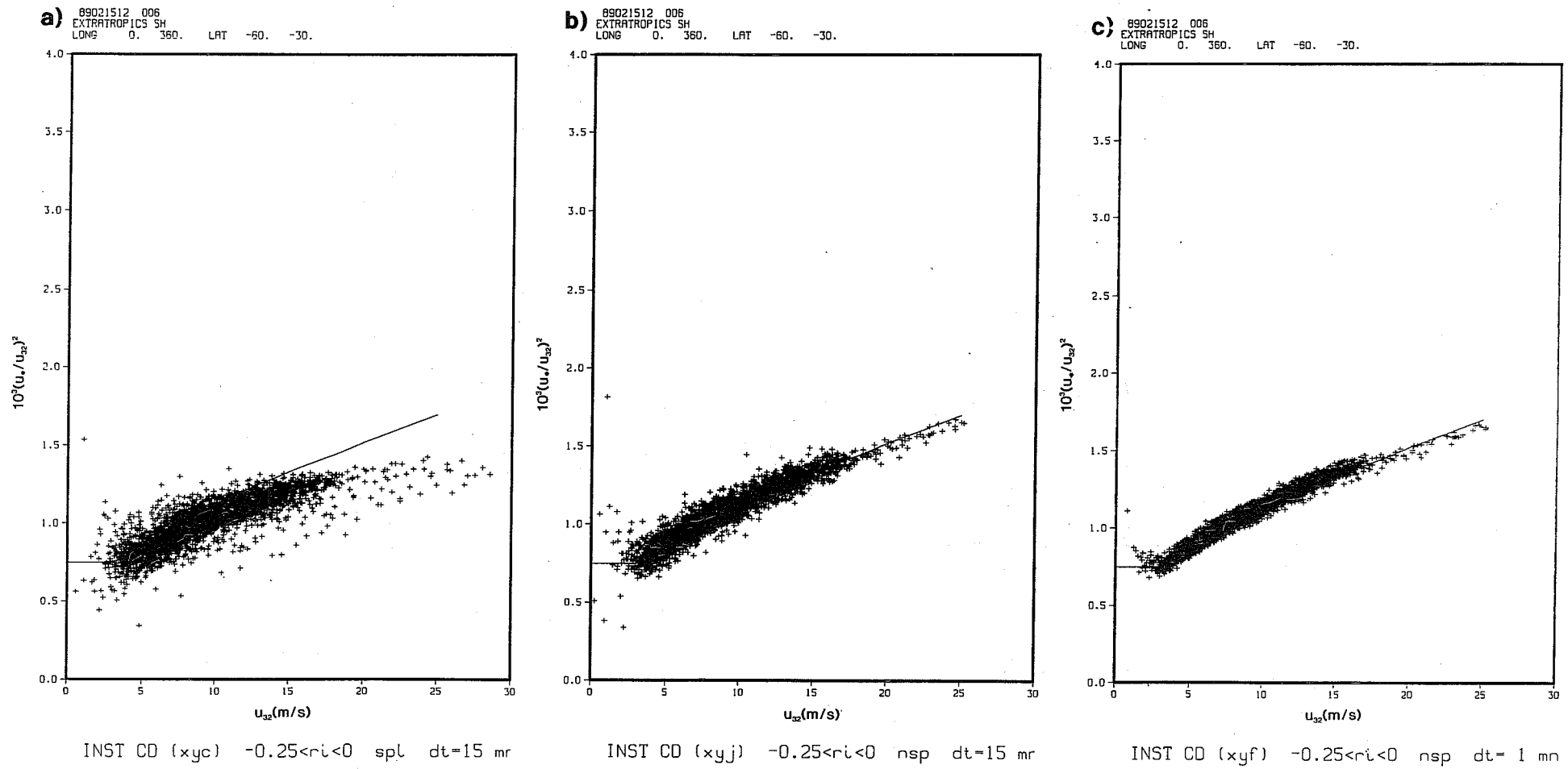

Fig. 11 Drag coefficients derived from model surface winds and surface stresses of all grid points over ocean at the Southern hemisphere where the bulk Richardson number between the surface and the lowest model level is between -0.25 and 0. A: process splitting, $2\Delta t$=1800 s; B: fractional steps, $2\Delta t$=1800 s; C: fractional steps, $2\Delta t$=120 s. The solid line represents the drag coefficient imposed by the neutral part of the parametrization.

$$K_M = K_H = \ell^2 \left|\frac{\partial U}{\partial z}\right| \; (1 + b\,|Ri|)^n \;,$$

$$Ri = \frac{g}{\theta} \frac{\partial\theta/\partial z}{(\partial U/\partial z)^2 + (\partial V/\partial z)^2} \;. \qquad (33)$$

One way of stabilizing the numerical solution is by linearizing the equations in U and θ and treating all linear terms implicitly. The drawback is that the equations for U, θ are coupled now, and instead of solving two tridiagonal problems we have to solve a single band matrix with a width of 6. In a real atmospheric model with equations for U, V, θ and q this would imply a band matrix with 12 diagonals. Another disadvantage is that through the complication of the algebra, the flexibility in closure is lost.

A simple stable scheme can be constructed by using the implicitness factor α (see eq. 27). This idea was introduced in the ECMWF model when stability problems became evident with the increase of horizontal resolution from T63 to T106 (Jarraud et al. 1985). The exchange coefficients are evaluated at time level n-1, but for the linear part of the diffusion term we use a weighted average between time level n-1 and n+1 (see eq. 28). With α=1, we would have a fully implicit scheme, but due to non-linear effects this scheme is not always stable. In the ECMWF T106L19 model coefficient α is 1.5. Girard and Delage go up to values of 4 which is very detrimental to the time truncation errors, but they propose to let it depend on local conditions. Dependent on a local stability criterion they select values between 0.5 and 4, which implies second order accuracy where the stability criterion allows it and very poor accuracy where the stability requirements are very restrictive.

A stability analysis for a variety of numerical schemes applied to a one layer non-linear model was published by Kalnay and Kanamitsu (1988). They also investigate the "explicit coefficient extrapolated Ψ" scheme with variable α. Their simple non-linear equation reads

$$\frac{\partial\Psi}{\partial t} = -(K\Psi^P)\;\Psi \;, \qquad (34)$$

$$\frac{\Psi_{n+1} - \Psi_{n-1}}{2\Delta t} = -K\,\Psi_{n-1}^{P}\,\{\alpha\Psi_{n+1} + (1-\alpha)\Psi_{n-1}\}\,, \qquad (35)$$

where double time steps are used for consistency with the previous equations. The amplification factor is

$$\frac{1 - q(P+1-\alpha)}{1 + q\alpha}\,, \text{ where } q = 2\Delta t\, K\, \Psi^{P}, \qquad (36)$$

which is smaller then 1 and larger than -1 for $q(P+1-2\alpha) < 2$. So we see that dependent on the degree of non-linearity as expressed by exponent P we can select α to satisfy the stability criterion. In the one column calculations with the ECMWF 19 level resolution in section 4.1, a value of 1.5 was used for α, but it had to be increased to 2 for the high resolution integrations.

The stability problems with the vertical diffusion scheme are very much connected to the closure scheme. The reason for the instability is the dependence of the exchange coefficients on the gradients of wind and temperature. The instability occurs because oscillations are allowed in the profile of exchange coefficients. It may therefore be worth considering the scheme proposed by Troen and Mahrt (1986) and further developed by Holtslag et al.(1990), in which the profile of exchange coefficients is prescribed as a similarity function throughout the boundary layer. Preliminary tests in the ECMWF model have shown that this scheme is much more robust and remains stable with α=1.

4.4 Noise

Recently it was discovered that in the operational T106L19 model the surface fluxes of heat, moisture were sometimes noisy. When the noise occurred, all the physic tendencies became noisy, particularly in the boundary layer. An example is shown in Fig. 12a for the South Pacific. The period of the noise is $4\Delta t$ (which implies 2 time steps for the physics) and this suggests a stability problem of the type described in the previous section. Increasing α to a value of 3 to stabilize the vertical diffusion scheme was

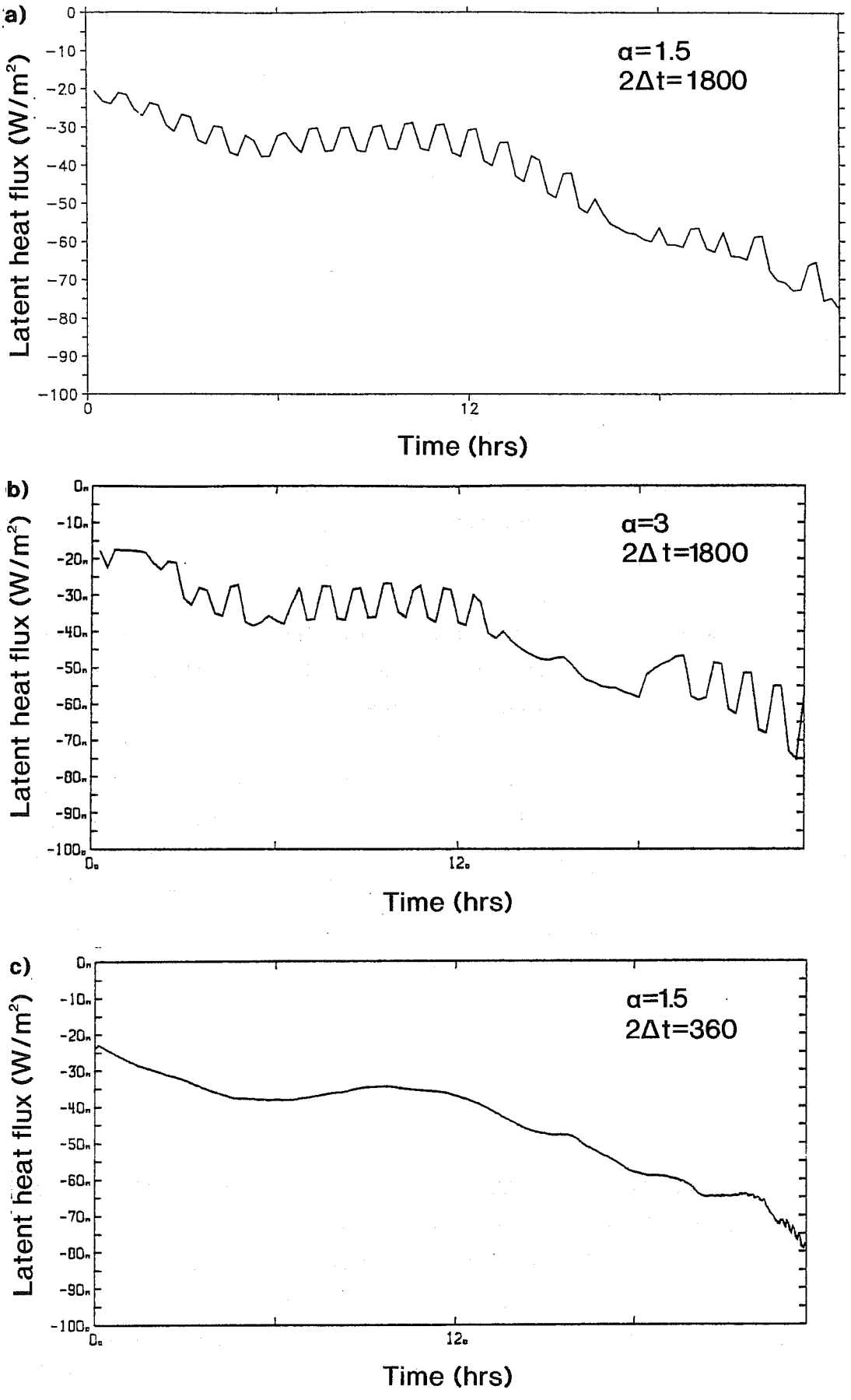

Fig. 12 Latent heat flux for a 24 hour forecast with T106L19 at 155 W 55 S from 15/7/90 12Z. a)operational model with α=1.5 and $2\Delta t$=1800 s; b)α=3 and $2\Delta t$=1800 s; c)αa=1.5 and $2\Delta t$=360.

initially tried. The noise pattern changed slightly (see Fig. 12b) but kept the same amplitude. Only a reduction of the time step from 15 minutes to 3 minutes eliminated the problem (Fig. 12c).

If the noise of Fig. 12 was related to the stability of the scheme, it should have responded to an increase of α in accordance with the analysis of Girard and Delage (1990) and Kalnay and Kanamitsu (1988). In reality the noise turns out to be due to an interaction of "process splitting noise" and the exchange coefficients in the vertical diffusion scheme. The vertical diffusion scheme does not produce the noise on its own, but interacts with other terms of the full equations.

To investigate the problem a little further the one column version of the vertical diffusion (see 4.1) has been applied on the situation with noise in the surface fluxes. The only modification is that extra tendencies were added to the θ-equation at the three lowest model levels. These tendencies were taken from the operational model with special diagnostics and are mainly due to advection. The tendencies are -2.94, 2.50 and -2.94 K/day for the three lowest model levels respectively. The mixed layer covers only three layers and has a depth of about 400 m. Fig. 13 shows that the simple one column model reproduces the oscillatory behavior of the surface heat flux. This is only the case if the extra (dynamics) tendencies are present in the equation for θ and when process splitting is applied. With the method of fractional steps, the noise disappears (see Fig. 13). The reason for the oscillations can be understood from the sequence of temperature profiles in Fig. 14, covering the time span of two time integration steps. The profiles of exchange coefficients and heat fluxes that correspond to these two time steps are shown in Fig. 15. In a convective boundary layer the vertical differences in potential temperature are extremely small; often less than 0.1 K between successive levels. This uniformity is created by the diffusion scheme because the exchange coefficients are very large in unstable situations. When after the diffusion step, another process causes differences in increments of e.g. 0.05 K between two levels, the layer between these two levels can change from slightly unstable to slightly stable. The diffusion coefficient for this layer, computed for the next time step, can become extremely small. In this way one layer can switch between stable and unstable every time step. When the method of fractional steps is used, the diffusion tends to smooth the noise

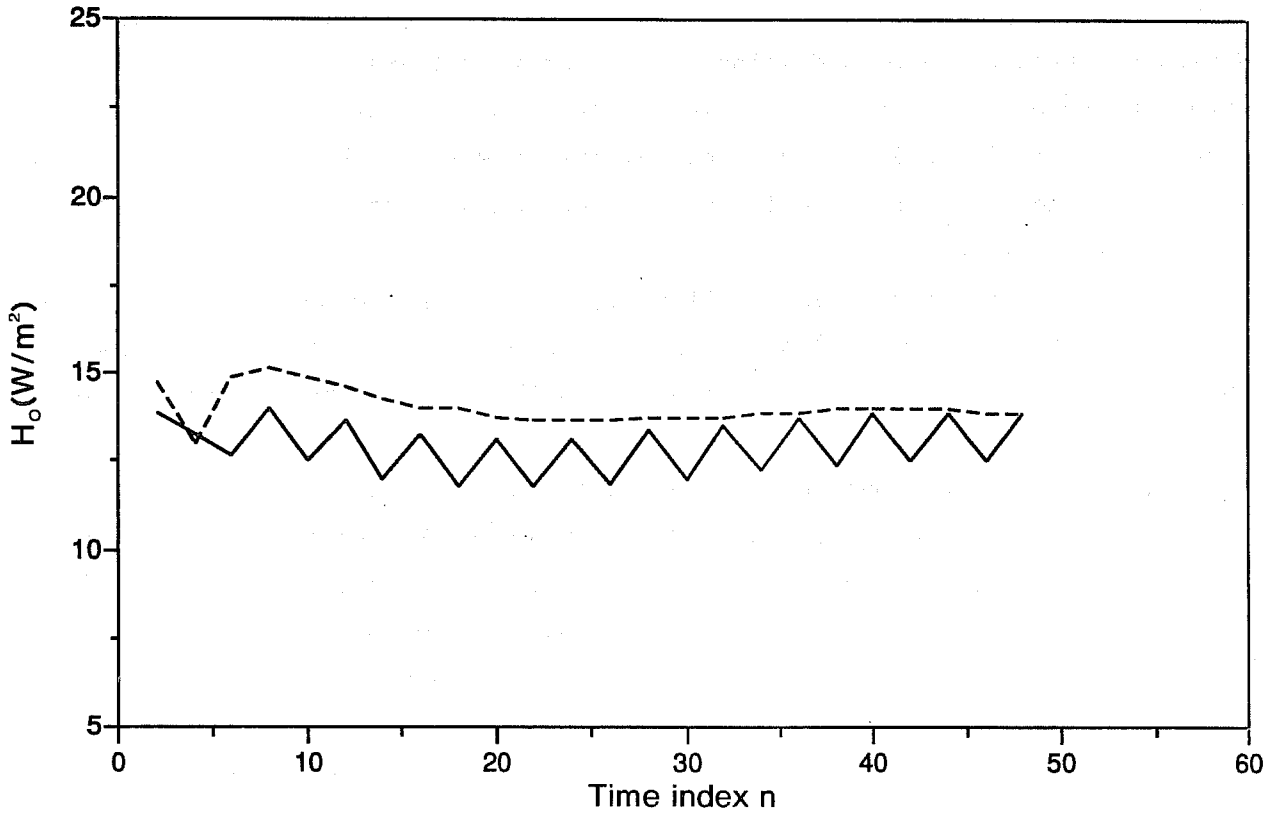

Fig. 13 Sensible heat flux with a one column version of the vertical diffusion code with tendencies of -2.94, 2.50 and -2.94 K/day added to the three lowest model levels. Two schemes are applied: process splitting (solid line) and fractional steps (dashed line).

created by the other terms in the same time step, so the input to the computation of the exchange coefficients will always be smooth.

The method of fractional steps works also better in the full three dimensional model as shown in Fig. 16a. Not all the oscillations have disappeared, because only the dynamics and the radiation tendencies are passed to the diffusion scheme. The convection and large scale precipitation cause also noise that interacts with the diffusion coefficients. This is mainly caused by the evaporation of precipitation in the lower layers.

From the examples shown here it is clear that the noise characteristics of the diffusion scheme are strongly related to the local closure. The alternative closure, that prescribes the profile of diffusion coefficients as similarity profile, is much more robust, also if combined with process splitting (see Fig. 16b).

5. SOIL PROCESSES

In the ECMWF model the surface boundary condition for temperature and the resistance for evaporation over land is provided by the land surface parametrization scheme (see Fig. 17). It consists of a three layer soil model with prognostic equations for temperature and soil moisture at the upper two layers and prescribed climate fields for the bottom layer. The climate fields are fixed per month. In this paper we limit the discussion to the temperature problem as the equations for moisture are very similar. The temperature in the soil is described by the diffusion equation

$$C_s \frac{\partial T}{\partial t} = K_T \frac{\partial^2 T}{\partial z^2} \quad . \tag{37}$$

or

$$C_s \frac{\partial T}{\partial t} = - \frac{\partial}{\partial z} H \quad , \text{ where } \quad H = -K_T \partial T / \partial z. \tag{38}$$

In these equations, H stands for the heat flux, C_s for the soil heat capacity and K for the thermal conductivity. The discretized forms for T_s and T_d are

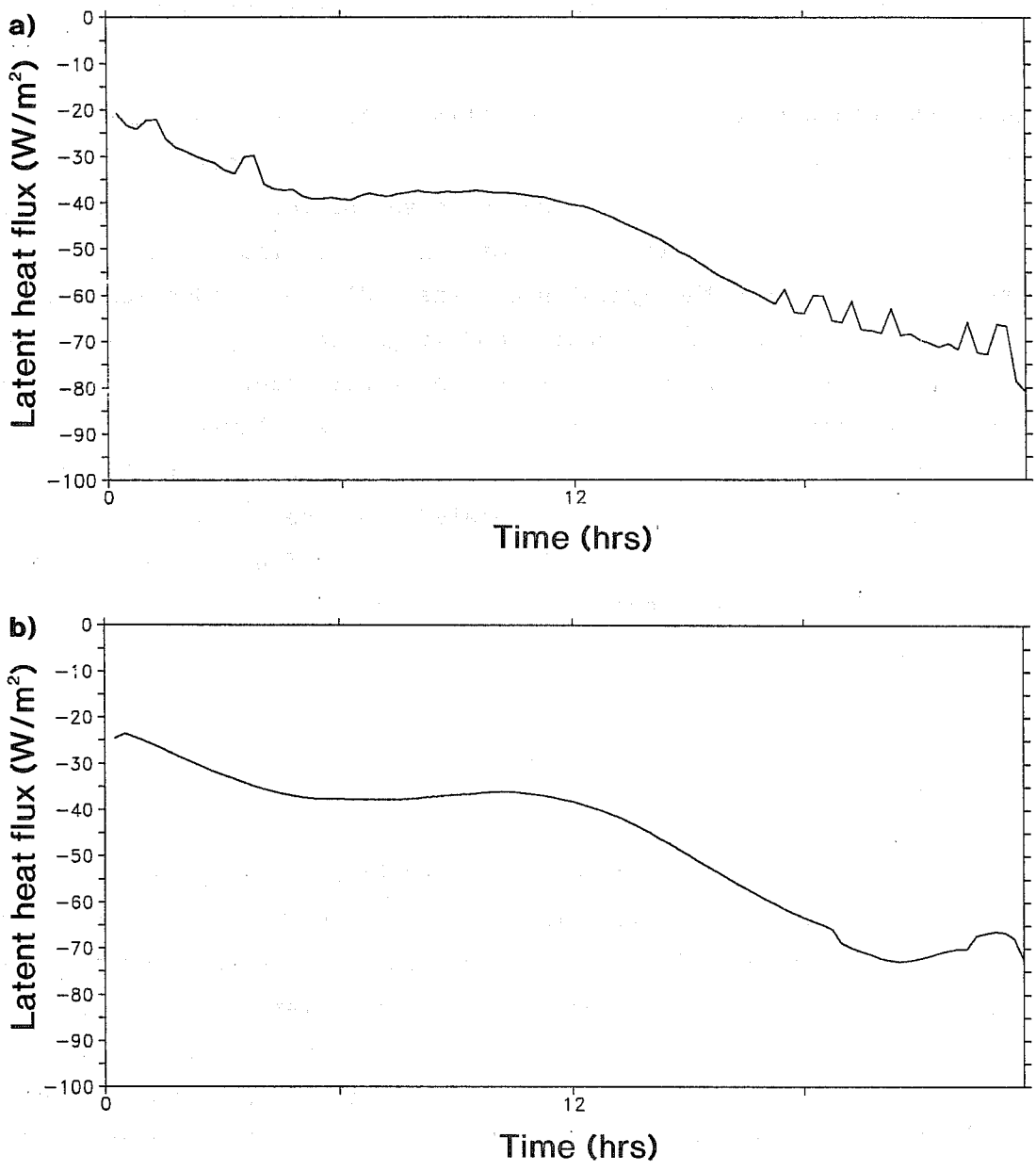

Fig. 16 As Fig 12a but with fractional steps(a) and with process splitting but with K-profile closure(b).

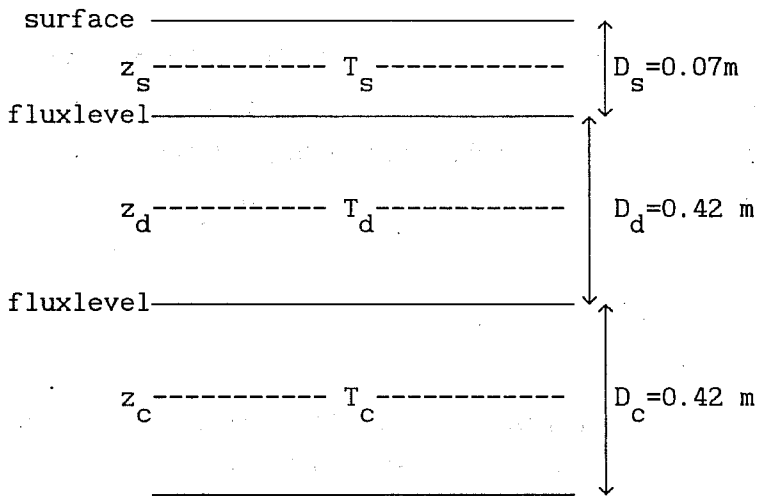

Fig. 17 Distribution of soil layers in the ECMWF model. The temperatures are defined in the middle of the layers. The top layer is called surface layer, the middle layer is called deep layer and the bottom layer is called climate layer.

$$C_s \frac{T_s^{n+1} - T_s^{n-1}}{2\Delta t} = - \frac{1}{D_s}\left\{ -K_T \frac{T_d^{n+1} - T_s^{n+1}}{0.5(D_s+D_d)} - H_o^{n+1} \right\} \tag{39}$$

$$C_s \frac{T_d^{n+1} - T_d^{n-1}}{2\Delta t} = - \frac{1}{D_d}\left\{ -K_T \frac{T_c^{n+1} - T_d^{n+1}}{0.5(D_d+D_c)} + K_T \frac{T_d^{n+1} - T_s^{n+1}}{0.5(D_s+D_d)} \right\} \tag{40}$$

where H_o^{n+1} is the soil heat flux at the surface from the atmospheric model (sensible plus latent heat flux plus net radiation). Since H_o depends on the surface temperature in the atmospheric model, it has to be treated implicitly. This is done by linearizing H_o with respect to T_s

$$H_o^{n+1} = H_o^{n-1} + \frac{dH_o}{dT_s}(T_s^{n+1} - T_s^{n-1}) \ . \tag{41}$$

The derivative of H_o with respect to T_s is computed in the boundary layer scheme for later use in the land surface scheme.

The numerical solution of the diffusion equation can not be expected to be accurate for all time scales with the resolution specified in Fig. 17. The choice of the number of layers and their thickness is very much inspired by the physical processes that need to be simulated. The depth of the surface layer has been chosen in accordance with the penetration depth of the diurnal temperature wave, the deep layer reflects changes on a time scale of the order of 10 days and the climate layer gives the seasonal variations. To investigate the accuracy of the numerical scheme we consider a sinusoidal boundary condition for the heat flux at the surface with frequency ω represented in complex form by

$$T_s = T_o \, e^{i\omega t} + T_c \ , \tag{42}$$

resulting in the analytical solution

$$T = T_o \, e^{i\omega t} \, e^{-(1+i)z/D} + T_c \ , \tag{43}$$

$$H_o = K_T \, T_o \, e^{i\omega t} \, \frac{(1+i)}{D} \quad , \text{ where } D = \left\{ \frac{2K_T}{C_s \omega} \right\}^{1/2} \ . \tag{44}$$

The accuracy of the three layer model is illustrated in Fig.18 where amplitude and phase errors are given of the surface temperature T_s and the deep layer temperature T_d. These errors are obtained by solving the vertically discretized equations analytically, so the errors are due to vertical discretization only (see Warrilow et al. 1986). The amplitude ratio is the amplitude from the discretized problem divided by the exact solution. For the purpose of medium range forecasting one would like to have accurate results in the time range of a few hours to 10 days. The scheme gives reasonable results for the diurnal cycle, but performs best for time scales of 5 to 10 days. For short time scales (e.g. less than half a day) the errors are quite large. This is probably not so important for the surface temperature because the diurnal cycle determines the dominant time scale. For soil moisture however, the time scale imposed by precipitation can be much shorter.

6. CONCLUDING REMARKS

Recent research has shown that diabatic processes are important for medium range forecasting. Improvements were obtained by better representation of different sub-grid processes, but little attention has been paid to the numerical aspects of the parametrizations. In this paper an overview of the numerics of parametrized processes has been given. Although the arguments and material, presented in this paper, have been derived from the ECMWF model, they probably apply to many other models as well.

One of the important numerical aspects of the ECMWF model is the leapfrog scheme, which implies that the total time path is integrated twice with double time steps. This scheme is second order accurate for the dynamics. Most parametrized processes however are parabolic in nature rather than hyperbolic and therefore the leapfrog scheme is not suitable. Forward or backward schemes are used instead, implying that the schemes for the parametrized processes are first order accurate only. Replacement of the leapfrog scheme with a two time level scheme would be more satisfactory.

A second aspect, that has been addressed, is the process splitting procedure versus fractional steps. The conclusion is that, with time steps

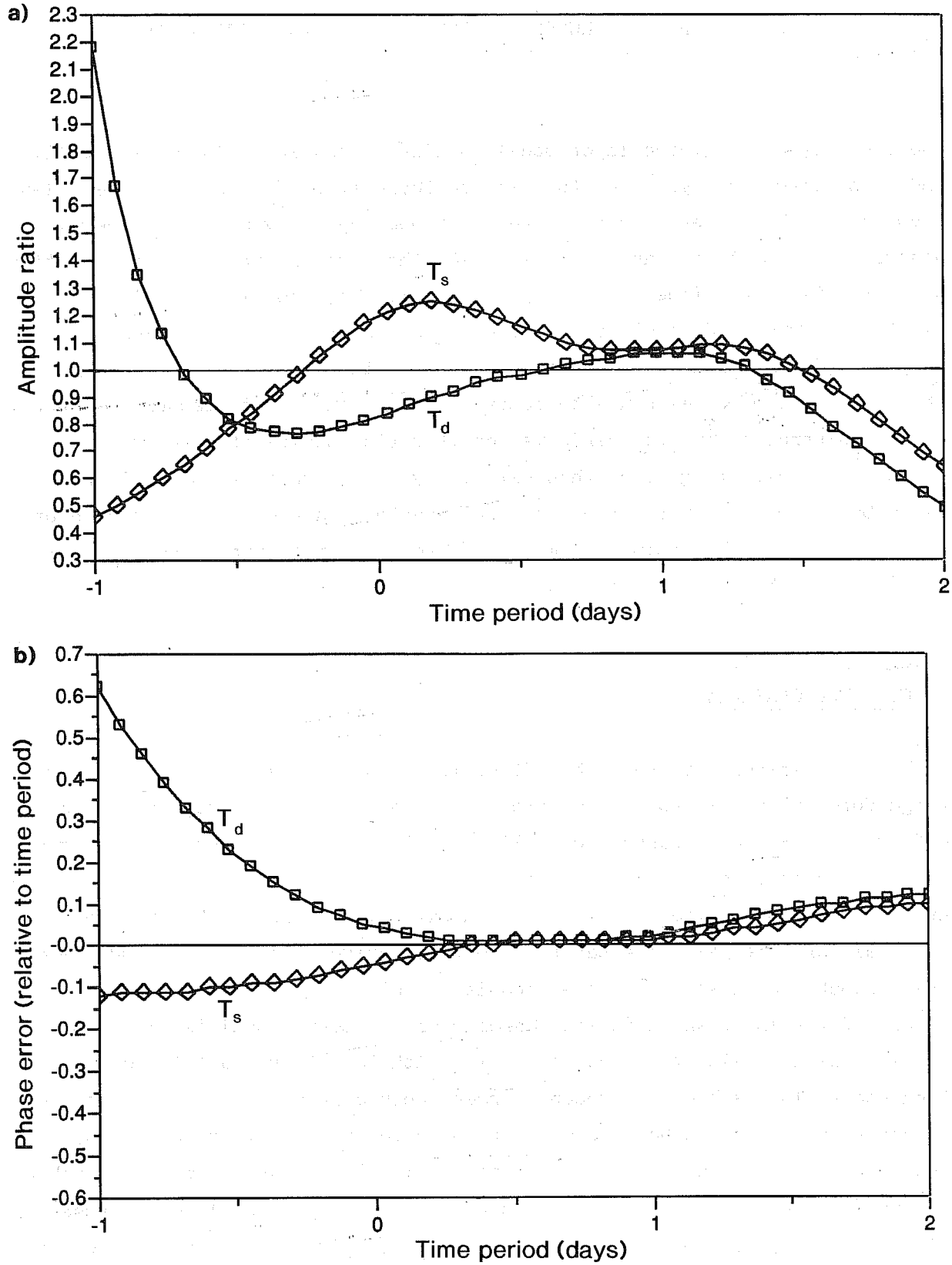

Fig. 18 Amplitude ratio (a) and phase errors (b) as a function of the period of the forcing (in days). A harmonic forcing is applied to the heat flux H at the surface. Errors are give for the surface temperature and the the deep temperature at z=0.245 m and are relative to the analytical solution.

long compared to the time scale of a process, it is beneficial to update the n-1 fields with the slower processes before treating the fast process implicitly. This principle has been illustrated with the vertical diffusion scheme. When the n-1 fields are updated with the dynamic tendencies before applying the diffusion, systematic errors in the surface wind are reduced and some of the noise problems disappear. The general idea is that with longer time steps it becomes more and more relevant to keep an accurate balance between processes within a single time steps. The general recipe is to order the processes according to their time scale: first the slow (explicit) processes then the faster processes (implicit) with updated n-1 fields and finally the adjustment processes.

With the availability of more and more computer power the scales that can be resolved by atmospheric models are becoming smaller. Consequently there is a danger that some processes are partially resolved as well as parametrized. This is already seen for orographic gravity waves (lee waves) whose scales are increasingly resolved by high resolution forecast models (e.g. T213). With further increasing resolution this will also be the case for convection, and it may already be so for slantwise convection. It is obvious that the parametrization problem becomes more complicated when there is no clear separation of scales. This will be a major topic of research in future fine-mesh models.

Another important topic of research with complicated numerical aspects will be cloud parametrization. Stratocumulus clouds for instance can be shallow (a few hundred meters deep) and have sharp upper and lower boundaries associated with a strong inversion, radiative flux divergence and turbulent fluxes. Higher vertical resolution is obviously needed, but will probably never be sufficient to resolve these processes in a satisfactory way. It will therefore be necessary to pay special attention to the numerical schemes that are associated with cloud processes.

Acknowledgements

It is a pleasure to thank my colleagues at the ECMWF research department for the numerous discussions. The manuscript benefitted considerably from suggestions and comments by Martin Miller, Adrian Simmons, Michael Tiedtke and Pedro Viterbo.

References

Beljaars, A.C.M., and A.A.M. Holtslag, 1991: On flux parametrization over land surfaces for atmospheric models. J. Appl. Meteor., 30, 327-341.

Delage, Y. (1988): The position of the lowest levels in the boundary layer of atmospheric circulation models, Atmos. Ocean, 26, 329-340.

Girard, C. and Y. Delage, 1990: Stable schemes for the vertical diffusion in atmospheric circulation models, Moth. Weath. Rev., 118, 737-746.

Holtslag, A.A.M., E.I.F. De Bruin, and H.L. Pan, 1990: A high resolution air mass transformation model for short-range weather forecasting, Month. Weath. Rev., 118, 1561-1575.

Jarraud, M., A.J. Simmons, and M. Kanamitsu, 1985: Development of the high resolution model, ECMWF Tech. Memo No. 107, 61pp.

Kalnay, E. and M. Kanamitsu, 1988: Time schemes for strongly nonlinear damping equations, Month. Weath. Rev., 116, 1945-1958. Louis, J.F. (1979): A parametric model of vertical eddy fluxes in the atmosphere, Bound.-Layer Meteor., 17, 187-202.

Louis, J.F., M. Tiedtke and, J.F. Geleyn, 1982: A short history of the operational PBL-parameterization at ECMWF, Workshop on boundary layer parameterization, November 1981, ECMWF, Reading, England.

Tiedtke, M., 1989: A comprehensive mass flux scheme for cumulus parameterization in large-scale models, Month. Weath. Rev., 117, 1779-1800

Troen, I. and L. Mahrt, 1986: A simple model of the atmospheric boundary layer; sensitivity to surface evaporation, Bound.-Layer Meteor., 37, 129-148.

Warrilow, D.A., A.B. Sangster, and A. Slingo, 1986: Modelling of landsurface processes and their influence on European climate, DCTN 38, Met. Office,Bracknell.